REGENERATION

# CLIC5 promotes myoblast differentiation and skeletal muscle regeneration via the BGN-mediated canonical Wnt/β-catenin signaling pathway

**Xin Zhang[1,2]†, Linjuan He[1]†, Liqi Wang[1]†, Yubo Wang[1], Enfa Yan[1], Boyang Wan[1], Qiuyu Zeng[1], Pengguang Zhang[1], Xingbo Zhao[3], Jingdong Yin[1,2]***



**Myoblast differentiation plays a vital role in skeletal muscle regeneration. However, the protein-coding genes controlling this process remain incompletely understood. Here, we showed that chloride intracellular channel 5 (CLIC5) exerts a critical role in mediating myogenesis and skeletal muscle regeneration. Deletion of CLIC5 in skeletal muscle leads to reduced muscle weight and decreases the number and differentiation potential of satellite cells. In vitro, CLIC5 consistently inhibits myoblast proliferation while promoting myotube formation. CLIC5 promotes myogenic differentiation by activating the canonical Wnt/β-catenin signaling pathway in a biglycan (BGN)–dependent manner. CLIC5 deletion impairs muscle regeneration. Paired box gene 7 (Pax7) expression and the activity of BGN-mediated canonical Wnt/β-catenin signaling are reduced in CLIC5-deficient mice. Conversely, increasing CLIC5 levels in skeletal muscles enhances muscle regeneration capacity. In conclusion, our findings underscore CLIC5 as a pivotal regulator of myogenesis and skeletal muscle regeneration, functioning through interaction with BGN to activate the canonical Wnt/β-catenin signaling pathway.**

## INTRODUCTION

Skeletal muscles constitute approximately 35% of the body's weight and are crucial for support, locomotion, and metabolism (*1*, *2*). Impairments due to injury or aging substantially affect quality of life. As adult stem cells within skeletal muscle, muscle satellite cells (MuSCs) respond to the impairments by activating to proliferate, differentiate, and fuse to form new muscle fibers or to fuse with existing ones (*3*). This myogenic process, including myoblast proliferation and differentiation, is essential not only for muscle development and growth but also for effective muscle regeneration.

Various cellular and molecular molecules induce myogenesis in muscle regeneration (*4*, *5*). Among these, several Wnt proteins are secreted (*6*). The canonical Wnt/β-catenin signaling pathway plays established roles in regulating myoblast differentiation (*7*–*10*), while its effect on myoblast proliferation remains debated (*11*, *12*). β-Catenin, a central component of canonical Wnt signaling, can be degraded by a complex including axins, adenomatous polyposis coli, casein kinase I, and glycogen synthase kinase–3β (GSK-3β). Wnt ligands induce the breakdown of the β-catenin degradation complex, causing the accumulation and movement of active β-catenin to the nucleus, which affects the expression of myogenic regulatory factors (*13*). Recent studies have revealed that secreted proteins and long noncoding RNAs can modulate the Wnt canonical signaling pathway during myogenesis (*14*, *15*). However, the specific Wnt signaling regulators affecting myoblast proliferation and differentiation remain largely unknown.

Chloride intracellular channel 5 (CLIC5), a member of the CLIC protein family, has natural mutants linked to hearing and balance issues (*16*). A natural deletion mutation in exon 5 of the CLIC5 restrained energy excess–induced obesity in mice (*17*). Our study in pigs revealed that CLIC5 overexpression inhibits preadipocyte adipogenic differentiation (*18*) while promoting myoblast myotube formation (*19*), but the role of CLIC5 in myogenesis remains mysterious. Genome-wide CRISPR screens in human embryonic kidney (HEK) 293T cells and melatonin treatment in C2C12 myoblasts have revealed a significant association between the CLIC5 expression level and Wnt/β-catenin signaling activity (*20*, *21*). This indicates that CLIC5 could be a key regulator of canonical Wnt/β-catenin signaling, particularly during myogenesis. Accordingly, we explored the role of CLIC5 in myogenesis and muscle regeneration in the present study. Conditional CLIC5 deletion in skeletal muscle reduces muscle weight, impairs differentiation capacity of MuSCs, and leads to MuSCs exhaustion in vivo. Importantly, CLIC5 deletion impairs muscle regeneration, while CLIC5 overexpression in skeletal muscle accelerates after injury regeneration. Mechanistically, CLIC5 acts as a positive regulator of canonical Wnt/β-catenin signaling though interacting with biglycan (BGN) to promote myogenesis.

## RESULTS

### Loss of CLIC5 reduces muscle weight and decreases the number and differentiation potential of satellite cells

We studied the role of CLIC5 in myogenesis in vivo by breeding mice with a floxed *CLIC5* allele, featuring two loxP sites around exon 2, with transgenic mice that expressed Cre recombinase under the *Myf5* promoter. This breeding resulted in *CLIC5*-Flox;*Myf5*-Cre$^{+/-}$ (CLIC5$^{MKO}$) mice (fig. S1A). Mice with floxed CLIC5 alleles that did not express Cre recombinase (*CLIC5*-Flox;*Myf5*-Cre$^{-/-}$ mice)

[1]State Key Laboratory of Animal Nutrition and Feeding, College of Animal Science and Technology, China Agricultural University, Beijing 100193, China. [2]Frontier Science Center of Molecular Design Breeding, Ministry of Education, Beijing 100193, China. [3]National Engineering Laboratory for Animal Breeding, Key Laboratory of Animal Genetics, Breeding and Reproduction, Ministry of Agriculture and Rural Affairs, College of Animal Science and Technology, China Agricultural University, Beijing 100193, China.
*Corresponding author. Email: yinjd@cau.edu.cn
†These authors contributed equally to this work.

were used as controls, hereafter referred to as wild-type (WT) mice. Quantitative polymerase chain reaction (qPCR) analysis revealed a reduction in *CLIC5* expression in the tibialis anterior (TA), extensor digitorum longus, and gastrocnemius (GAS) ($P < 0.05$), while no significant changes were observed in other tissues, such as the soleus, epididymal white adipose tissue, inguinal white adipose tissue, liver, and spleen (fig. S1B). With the exception of the decreased *CLIC3* expression observed in the TA of CLIC5$^{MKO}$ mice, the mRNA expression levels of other CLIC family members in the TA, GAS, and extensor digitorum longus did not exhibit significant differences between WT and CLIC5$^{MKO}$ mice (fig. S1, C to E).

The CLIC5$^{MKO}$ mice were fertile and healthy. In particular, we observed that conditional knockout (KO) of CLIC5 resulted in reduced body weight in male and female mice since 3 weeks of age (Fig. 1, A and B). At 9 weeks of age, CLIC5 KO resulted in a 9.67 and 5.55% reduction in body weight in male and female mice, respectively. As CLIC5 KO has a more pronounced effect on body weight in male mice, male mice were used in the subsequent analysis. To investigate whether this decrease in body weight was associated with decreased muscle mass, we examined various skeletal muscles and found that the TA and GAS muscles in adult CLIC5$^{MKO}$ mice were lighter than those of age-matched WT mice ($P < 0.01$; Fig. 1, C and D). To validate the effect of CLIC5 regulation on MuSCs function, we isolated MuSCs using fluorescence-activated cell sorting (FACS) (Fig. 1E). The proportion of MuSCs was significantly decreased from 11.15 to 8.22% in the hind limbs of CLIC5$^{MKO}$ mice ($P < 0.01$; Fig. 1F). A 26.55% reduction in MuSCs was consistently observed in cross sections of the TA muscle (Fig. 1, G and H). We also found that CLIC5 KO reduced the percentage of 5-ethynyl-2′-deoxyuridine (EdU)–positive MuSCs (fig. S2, A and B) and decreased the mRNA levels of *p21* and key cell cycle–related genes, including cyclin D1 (*CCND1*) and cyclin-dependent kinase 2 (*CDK2*) ($P < 0.05$; fig. S2C), suggesting that CLIC5 KO reduces the proliferation of MuSCs.

In addition, we observed a limited number of myosin-positive multinucleated myotubes at day 3 following the myogenic induction of MuSCs isolated from CLIC5$^{MKO}$ mice (Fig. 1I). Consistently, the differentiation and fusion indices were significantly lower than those of WT MuSCs (Fig. 1J). Furthermore, qPCR analysis revealed a significant decrease in the mRNA expression levels of myogenic factor 5 (*Myf5*), myogenic differentiation antigen (*MyoD*), myogenin (*MyoG*), and *Myomaker* in CLIC5$^{MKO}$ MuSCs at day 1 of differentiation; however, these gene levels exhibited a significant increase at day 3 of differentiation (Fig. 1K). Western blotting revealed a significant decrease in the protein level of MyoG in CLIC5$^{MKO}$ MuSCs at day 2 but not at day 3 of differentiation (Fig. 1, L and M). This suggests that the differentiation and fusion of MuSCs might be delayed rather than completely blocked in the absence of CLIC5. As expected, further culturing in differentiation medium (DM) for an additional 2 days enabled CLIC5$^{MKO}$ MuSCs to differentiate into WT MuSCs (fig. S3).

## CLIC5 mediates the balance of proliferation and differentiation of myoblasts

To analyze the function of CLIC5 in myogenic differentiation, we examined the subcellular localization and temporal expression pattern of CLIC5 in vitro myogenesis system. We observed specific expression of CLIC5 in the cytoplasm of C2C12 myoblasts, with no nucleus presence (fig. S4, A and B). Throughout myogenic differentiation, mRNA and protein levels of CLIC5 increased, similar to the expression patterns of key myogenic markers, such as MyoG, Myomaker, and myosin (fig. S4, C to E).

To validate the role of CLIC5 in myogenic differentiation, we conducted CLIC5-knockdown experiments in C2C12 myoblasts. CLIC5 knockdown significantly increased the percentage of EdU-positive cells (Fig. 2, A and B). Furthermore, flow cytometry analysis showed that CLIC5 knockdown significantly reduced cell cycle arrest at $G_0$-$G_1$, decreased the percentage of S phase populations, and increased the percentage of $G_2$ phase populations ($P < 0.01$; Fig. 2C). Consistent with the cell cycle analysis, mRNA expression levels of *p21*, *CCND1*, cyclin E1 (*CCNE1*), and *CDK6* were significantly elevated in CLIC5-knockdown myoblasts compared to those of the control ($P < 0.05$ or $P < 0.01$; Fig. 2D). We further investigated the effect of CLIC5 knockdown on myoblast differentiation, observing shorter myosin-positive myotubes with fewer nuclei (Fig. 2E) and significantly reduced differentiation and fusion indices ($P < 0.01$; Fig. 2F). These observations were further supported by the decreased protein levels of myosin at day 4 of myoblast differentiation ($P < 0.05$; Fig. 2G), while the protein levels of MyoG remained unchanged (Fig. 2G). Similarly, the inhibition of CLIC5 by IAA94 (100 μM), a high-affinity ligand for chloride channel, also promoted proliferation and inhibited differentiation of C2C12 myoblasts, as revealed by EdU assay, cell cycle analysis, qPCR, and immunofluorescence of myosin (fig. S5). These findings suggest that CLIC5 inhibits myoblast proliferation while promoting myogenic differentiation and myotube formation.

Gain-of-function assay was also performed by stably overexpression of CLIC5 in C2C12 myoblasts. In contrast to CLIC5 knockdown or chemical inhibition, CLIC5 overexpression significantly reduced the percentage of EdU-positive cells (Fig. 2, H and I), led to cell cycle arrest at $G_0$-$G_1$ ($P < 0.01$; Fig. 2J), reduced the percentage of S and $G_2$ phase populations ($P < 0.01$; Fig. 2J), and suppressed the expression of *p21*, *CCNE1*, *CDK2*, and *CDK6* ($P < 0.01$; Fig. 2K). CLIC5-overexpressing myoblasts exhibited significantly enhanced formation of multinucleated myotubes (Fig. 2, L and M) and increased levels of MyoG and myosin (Fig. 2N) compared to the control at day 4 of differentiation. Collectively, these findings suggest the critical role of CLIC5 in maintaining a balance between myoblast proliferation and differentiation.

## Loss of CLIC5 impairs myoblast differentiation and canonical Wnt/β-catenin signaling

To investigate the mechanism of CLIC5 in myoblast differentiation, we used CRISPR-Cas9 editing to create CLIC5-KO C2C12 myoblasts. WT C2C12 myoblasts were induced to differentiate, whereas KO myoblasts showed a failure to differentiate (Fig. 3, A to D). Subsequently, we conducted RNA sequencing (RNA-seq) analysis on WT and KO myoblasts in proliferation. Briefly, a total of 396 genes with $P < 0.05$ and a fold change of $\geq 3$ or $\leq 0.33$ between WT and KO myoblasts were identified as differentially expressed genes (DEGs), including 171 up-regulated genes and 225 down-regulated genes in KO cells. In addition, 11 DEGs were randomly selected to validate the accuracy of RNA-seq using qPCR (Fig. 3E). Overall, 25 signaling pathways were significantly enriched on the basis of the DEGs (table S1), including pathways closely linked to myoblast differentiation, such as the Wnt signaling pathway ($q = 0.034$),

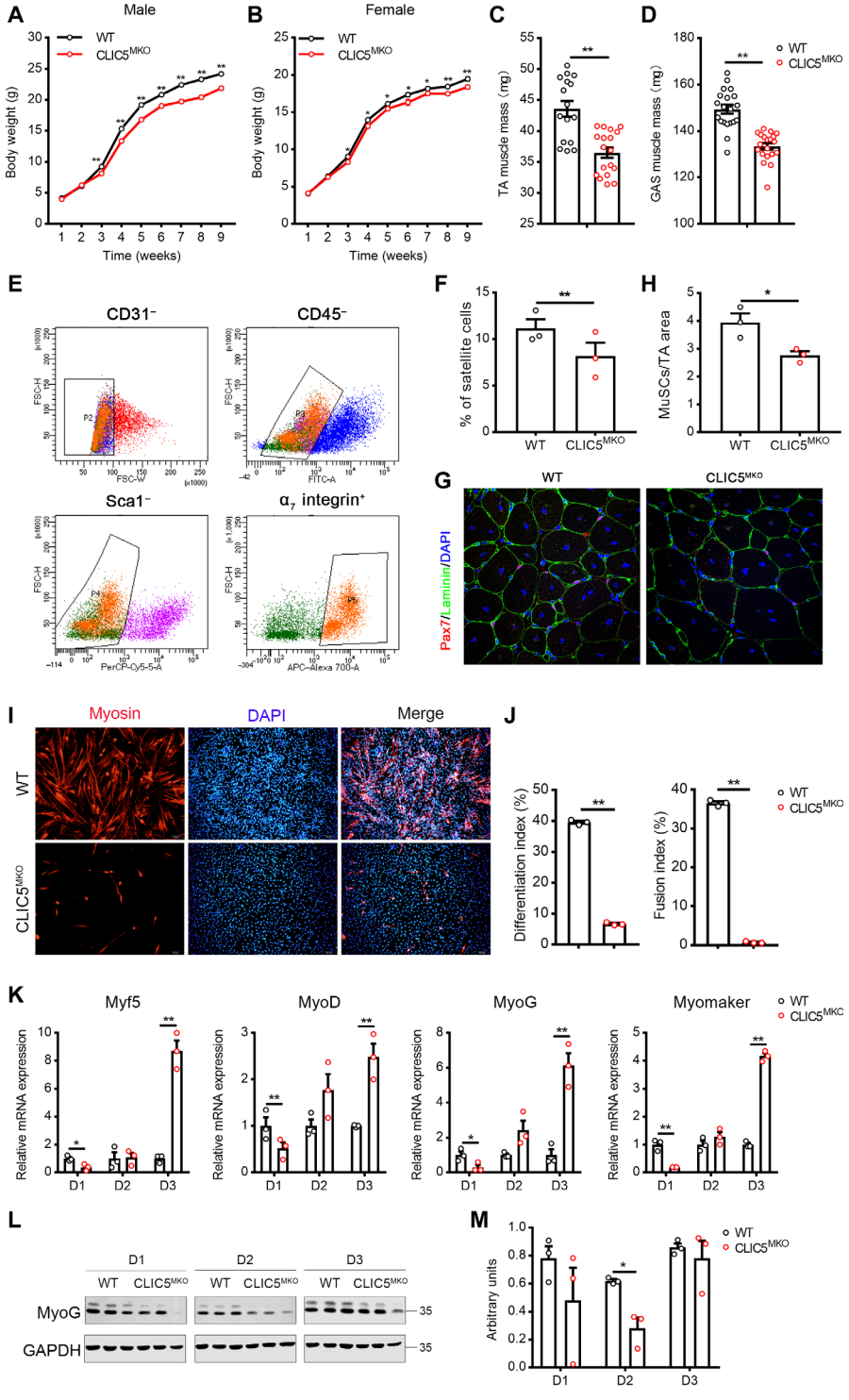


**Fig. 1. Loss of CLIC5 reduces muscle weight and decreases the number and differentiation potential of satellite cells.** Body weight of (**A**) male and (**B**) female mice from the age of 1 to 9 weeks. Muscle mass of (**C**) TA and (**D**) GAS in adult WT and CLIC5$^{MKO}$ mice. (**E**) Flow cytometry analysis of CD31, CD45, Sca1, and $\alpha_7$ integrin expression in whole musclve–derived cells. APC, allophycocyanin; FITC, fluorescein isothiocyanate; FSC-H, forward scatter height; FSH-W, forward scatter width; P2, CD31$^-$ cell populations. (**F**) The percentage of satellite cells in whole muscle–derived cells revealed by flow cytometry analysis. (**G** and **H**) Immunofluorescence of Pax7 and Laminin and satellite cells per area of TA muscle cross sections. Magnification, ×60. (**I**) Immunofluorescence analysis for myosin in satellite cells cultured for 3 days in DM. Magnification, ×10. (**J**) Differentiation index and fusion index. Differentiation index is calculated as the percentage of nuclei in myosin$^+$ cells. Fusion index is calculated as the percentage of nuclei in myosin$^+$ myotubes. Structures containing at least two nuclei are considered as a myotube. (**K**) Relative mRNA levels of Myf5, MyoD, MyoG, and Myomaker and (**L** and **M**) Western blot analysis of MyoG in satellite cells cultured in DM for 1, 2, or 3 days (D1, D2, or D3). GAPDH, glyceraldehyde-3-phosphate dehydrogenase. $n = 16$ to 20 for (A) to (D) and 3 for (E) to (M). The data present means ± SEM. *$P < 0.05$ and **$P < 0.01$.

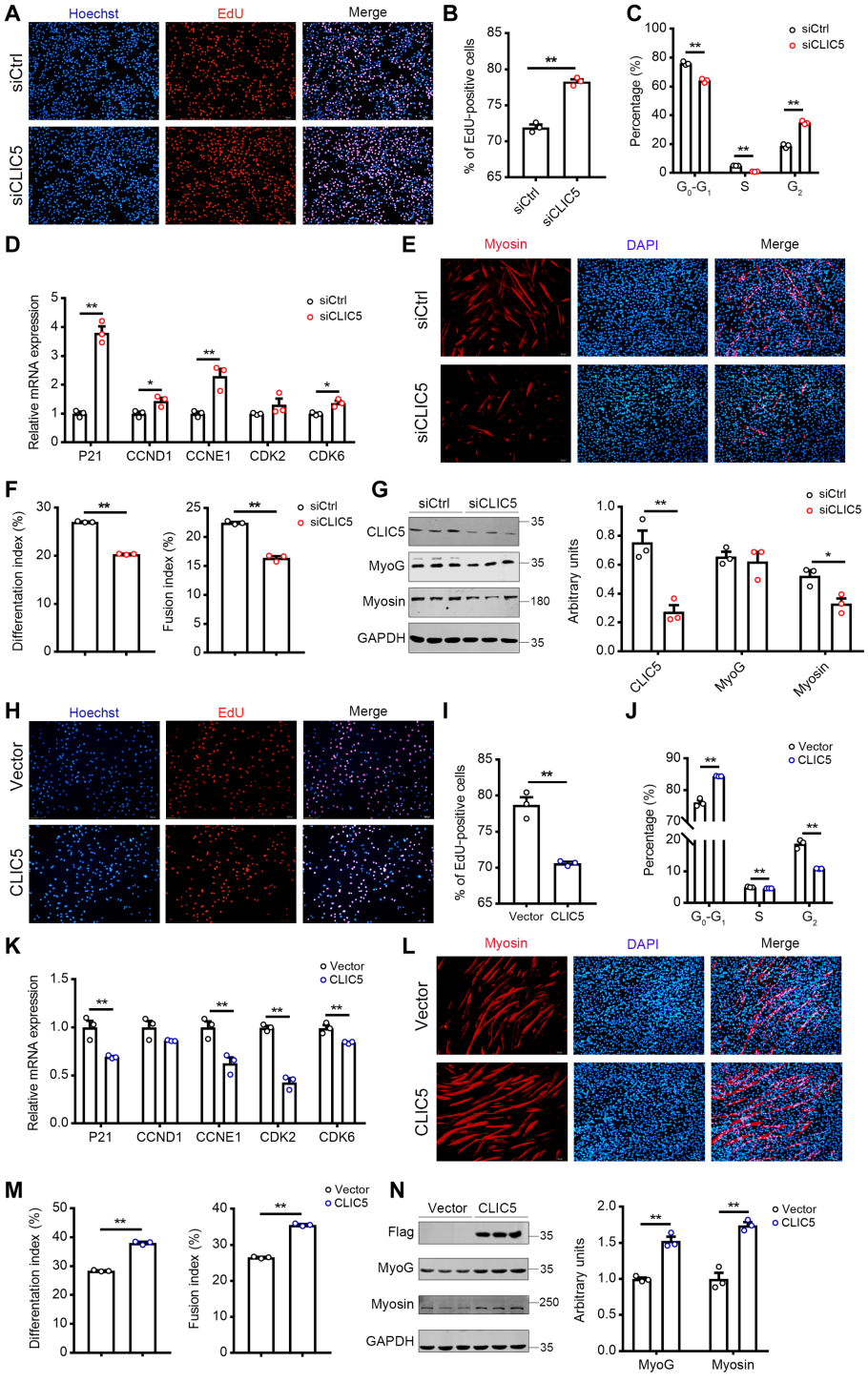


**Fig. 2. CLIC5 mediates the balance of proliferation and differentiation of myoblasts.** (**A** and **B**) Representative photographs of EdU staining in control (siCtrl) and CLIC5 knockdown (siCLIC5) C2C12 myoblasts. Nuclei were stained with Hoechst. Magnification, ×10. (**C**) Cell cycle analysis of siCtrl and siCLIC5 C2C12 myoblasts via flow cytometry. (**D**) Expression analysis of cell cycle–related genes in siCtrl and siCLIC5 myoblasts cultured in growth medium. (**E**) Immunofluorescence analysis for myosin in siCtrl and siCLIC5 C2C12 myoblasts after 4 days in DM. Magnification, ×10. (**F**) Differentiation index calculated as the percentage of nuclei in myosin$^+$ cells and fusion index calculated as the percentage of nuclei in myosin$^+$ myotubes. Structures containing at least two nuclei are considered as a myotube. (**G**) Western blot analysis of CLIC5, MyoG, and myosin in siCtrl and siCLIC5 C2C12 myoblasts after 4 days in DM. (**H** and **I**) Representative photographs of EdU staining in control (vector) and CLIC5-overexpressing C2C12 myoblasts. Nuclei were stained with Hoechst. Magnification, ×10. (**J**) Cell cycle analysis of control and CLIC5-overexpressing C2C12 myoblasts. (**K**) Expression analysis of cell cycle–related genes in control and CLIC5-overexpressing C2C12 myoblasts cultured in growth medium. (**L**) Immunofluorescence analysis for myosin in control and CLIC5-overexpressing C2C12 myoblasts after 4 days in DM. Magnification, ×10. (**M**) Differentiation index and fusion index. (**N**) Western blot analysis of Flag, MyoG, and myosin in control and CLIC5-overexpressing C2C12 myoblasts after 4 days in DM. The data present means ± SEM ($n = 3$). *$P < 0.05$ and **$P < 0.01$.

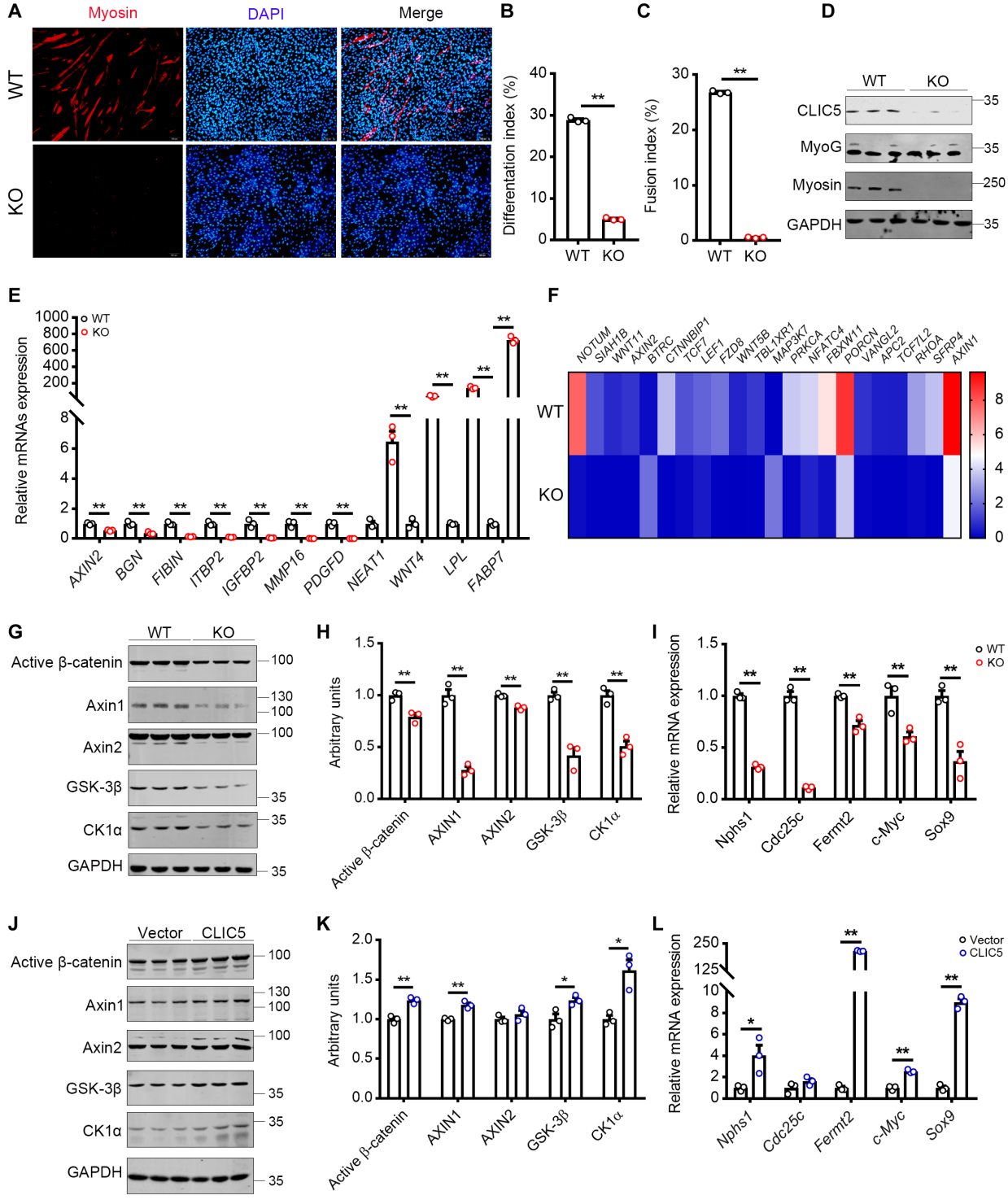


**Fig. 3. CLIC5 promotes myoblast differentiation and activates the canonical Wnt/β-catenin signaling pathway.** (**A**) Immunofluorescence analysis for myosin in WT and CLIC5-KO C2C12 myoblasts after 4 days in DM. Magnification, ×10. (**B**) Differentiation index. (**C**) Fusion index. (**D**) Western blot analysis of MyoG and myosin in WT and KO C2C12 myoblasts after 4 days in DM. (**E**) The mRNA expression levels of selected genes in WT and KO C2C12 myoblasts by RNA-seq. (**F**) Heatmap of DEGs enriched in Wnt signaling pathway in WT and KO C2C12 myoblasts. (**G** and **H**) Western blot analysis of active β-catenin, Axin1, Axin2, GSK-3β, and CK1α in WT and KO C2C12 myoblasts cultured in growth medium. (**I**) Relative mRNA levels of Wnt-targeted genes expressed in WT and KO C2C12 myoblasts. (**J** and **K**) Western blot analysis of active β-catenin, Axin1, Axin2, GSK-3β, and CK1α in control and CLIC5-overexpressing C2C12 myoblasts cultured in growth medium. (**L**) Relative mRNA levels of Wnt-targeted genes expressed in control and CLIC5-overexpressing C2C12 myoblasts. The data present means ± SEM ($n = 3$). *$P < 0.05$ and **$P < 0.01$.

Hippo signaling pathway ($q < 0.01$), ubiquitin-mediated proteolysis ($q < 0.01$), and phosphatidylinositol 3-kinase–Akt signaling pathway ($q = 0.011$).

Consistent with the reduced expression of most DEGs involved in the Wnt signaling pathway in KO cells (Fig. 3F), Western blot analysis revealed a significant down-regulation of active β-catenin, Axin1, Axin2, GSK-3β, and casein kinase 1α (CK1α) proteins in KO myoblasts (Fig. 3, G and H). Furthermore, the expression of Wnt target genes, such as nephrosis 1 (*Nphs1*), cell division cycle 25C (*Cdc25c*), fermitin family member 2 (*Fermt2*), *c-Myc*, and SRY-box transcription factor 9 (*Sox9*), was significantly decreased ($P < 0.01$; Fig. 3I). In contrast, CLIC5-overexpressing myoblasts showed increased levels of key components in the canonical Wnt/β-catenin pathway and elevated mRNA levels of Wnt target genes (Fig. 3, J to L). In addition, treatment with the Wnt activator, BML-284, significantly restored myotube formation and myosin expression in CLIC5-knockdown myoblasts (fig. S6). These results indicate that CLIC5 mediates proliferation and myogenic differentiation through the canonical Wnt/β-catenin signaling pathway.

### CLIC5 interacts with BGN to enhance myoblast differentiation and canonical Wnt/β-catenin signaling pathway

To understand how CLIC5 activates the canonical Wnt/β-catenin signaling pathway, we used mass spectrometry analysis by subjecting C2C12 cell samples to immunoprecipitation. This approach aimed to identify interaction partners of CLIC5 in myoblasts. The results revealed that BGN, an enhancer of canonical Wnt/β-catenin signaling (*22*), was a potential binding protein of CLIC5 (table S2). To confirm the association between CLIC5 and BGN, we investigated the cellular distribution of BGN in myoblasts. Immunofluorescence and fractionation of C2C12 myoblasts into nuclear and cytosolic fractions revealed that BGN was exclusively localized to the cytosolic fraction (Fig. 4, A and B). BGN and CLIC5 were both found in the cytoplasm (Fig. 4C). To further validate this interaction, we conducted an immunoprecipitation analysis and observed that CLIC5-Flag interacted with BGN-Myc (Fig. 4D). To identify the binding domain between CLIC5/BGN, we cotransfected HEK293T cells with plasmids encoding full-length CLIC5 or three different C-terminal truncated CLIC5s with BGN–hemagglutinin (HA). Our results indicated that $CLIC5^{1-196}$, $CLIC5^{1-137}$, and $CLIC5^{1-105}$ could pull down BGN similar to full-length CLIC5 (Fig. 4E). This indicates that residues 1 to 105 in CLIC5 are responsible for its binding to BGN, with this domain being crucial for the insertion of CLIC5 into the plasma membrane. The protein level of BGN decreased significantly by 34 and 65% in the cytosol and plasma membrane of CLIC5-KO C2C12 myoblasts, respectively (Fig. 4, F to H). Conversely, its level increased significantly upon CLIC5 overexpression (Fig. 4I). This indicates that CLIC5 binds to BGN and promotes its expression in myoblasts.

We then explored the role of BGN in myoblast differentiation and found that the expression pattern of BGN during myoblast differentiation mirrored that of CLIC5 (Fig. 5A). Knockdown of BGN in myoblasts resulted in inhibited myotube formation (Fig. 5B). These findings suggest that CLIC5 positively regulates myoblast differentiation through BGN. To validate this hypothesis, we examined the effect of CLIC5 knockdown on myoblast differentiation in the presence or absence of BGN. CLIC5 overexpression enhanced myotube formation in control small interfering RNA (siRNA)–transfected cells, while it did not have the same effect in BGN siRNA (siBGN)–transfected myoblasts (Fig. 5, C to E). Furthermore, CLIC5 did not enhance the canonical Wnt/β-catenin signaling pathway in the presence of siBGN (Fig. 5, F and G). Consistently, overexpression of BGN rescued defective differentiation (Fig. 5H) and restored canonical Wnt/β-catenin signaling in CLIC5-knockdown myoblasts after 6 days in DM (Fig. 5, I to K). These findings reveal that CLIC5 promotes myoblast differentiation and the canonical Wnt/β-catenin signaling pathway in a BGN-dependent manner.

### Loss of CLIC5 delays skeletal muscle regeneration

Histological analysis of TA muscles at days 3, 7, and 14 after injury was conducted to assess the role of CLIC5 in muscle regeneration (Fig. 6A). At day 3 after injury, WT mice exhibited newly formed muscle fibers, while $CLIC5^{MKO}$ mice showed minimal muscle fiber regeneration (Fig. 6B). At day 14 after injury, WT mice exhibited tightly packed, well-formed muscle fibers, while $CLIC5^{MKO}$ mice had fewer large muscle fibers (Fig. 6B). Furthermore, there were fewer newly formed myofibers at day 3, with more at day 7 after injury in $CLIC5^{MKO}$ regenerating muscles (Fig. 6C). These findings suggest that the absence of CLIC5 leads to delays in adult skeletal muscle regeneration. Consistent with the histological analysis, the protein levels of Pax7 and MyoG were reduced at day 3 after injury in the skeletal muscle of $CLIC5^{MKO}$ mice compared to those of WT mice ($P < 0.05$; Fig. 6, D and E), indicating a reduction in the number and differentiation potential of MuSCs. In addition, consistent with the results in vitro, the expression levels of BGN and the activity of canonical Wnt/β-catenin signaling pathway were significantly reduced in TA muscles of $CLIC5^{MKO}$ mice at day 3 after injury ($P < 0.05$ and $P < 0.01$; Fig. 6, D and E). These findings suggest that CLIC5 deficiency delays skeletal muscle regeneration through the BGN-mediated canonical Wnt/β-catenin signaling pathway.

We further tested whether loss of CLIC5 could repress BGN and Wnt/β-catenin signaling pathway in MuSCs. As shown in fig. S7, CLIC5 KO reduced protein levels of BGN, active β-catenin, axin2, and GSK-3β. Consistently, it also decreased expression levels of Wnt target genes, including *Nphs1*, *Cdc25c*, and *Sox9* (fig. S7C). Moreover, BML-284 treatment rescued myogenic differentiation in $CLIC5^{MKO}$ MuSCs, as evidenced by the increased mRNA levels of *Myf5*, *MyoD*, *MyoG*, and *Myomaker*, as well as the protein levels of MyoG and myosin (fig. S8). These findings suggest that CLIC5 also enhances myogenic differentiation in MuSCs by activating the canonical Wnt/β-catenin signaling.

### Increasing CLIC5 in the skeletal muscle enhances its regeneration capacity

Considering the negative effects of experimentally reducing CLIC5 protein levels on myogenic differentiation and muscle regeneration, we investigated the functional significance of CLIC5 during muscle regeneration. Cohorts of 8-week-old C57BL/6 mice were treated in TA by direct intramuscular injection with adeno-associated virus 9 (AAV9):CLIC5 or AAV9:empty vectors, and cardiotoxin (CTX) injection was conducted after 3 weeks of vector administration (Fig. 7A). Hematoxylin and eosin (H&E) staining of TA sections revealed that CLIC5 overexpression led to the replacement of most inflammatory myofibers with newly formed myofibers at day 7 following CTX injection. In contrast, control mice still exhibited more inflammatory cells and necrotic myofibers (Fig. 7B). This effect was consistent with

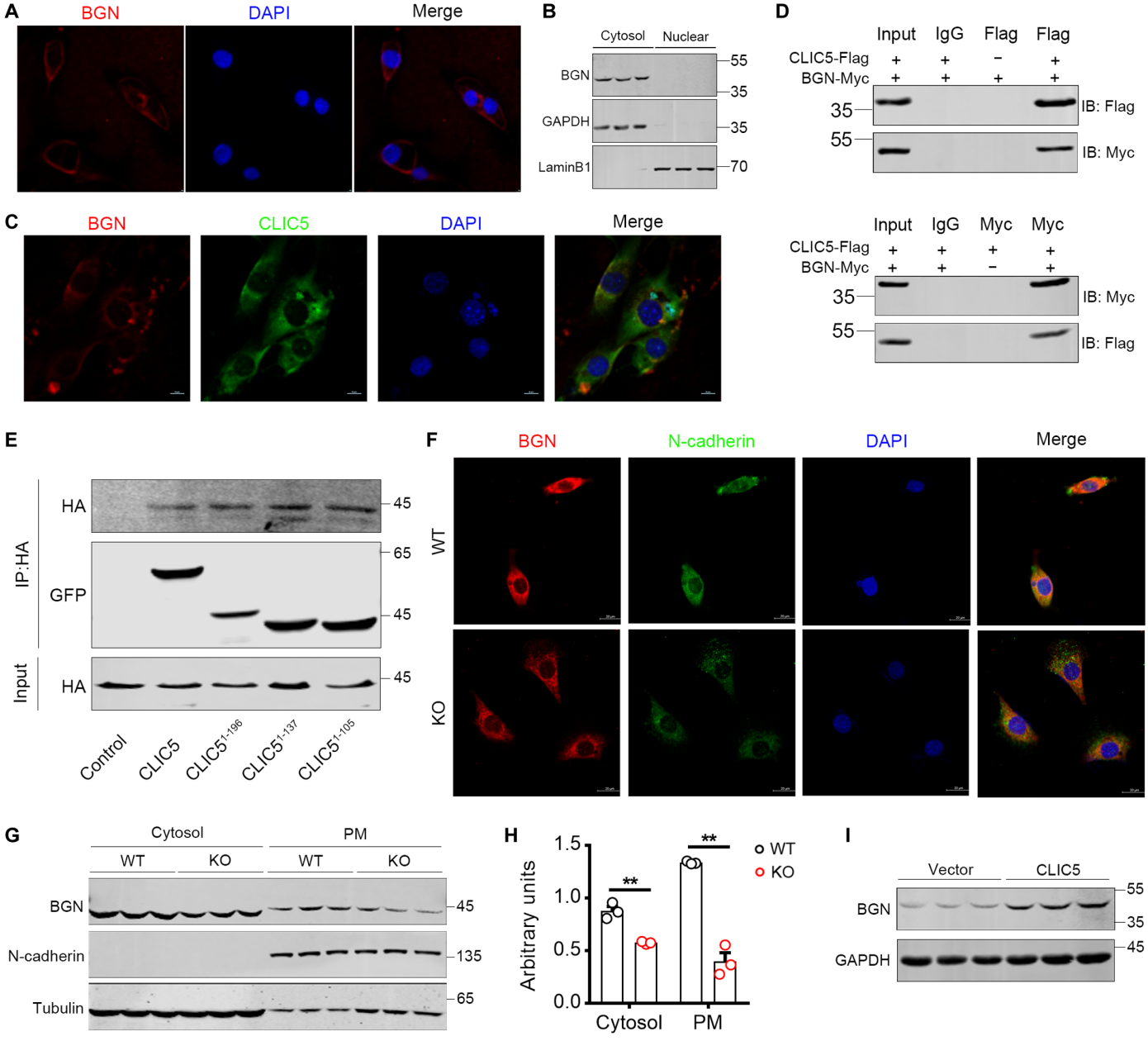


**Fig. 4. CLIC5 interacts with BGN and promotes its expression.** (**A**) Immunofluorescence staining of BGN in C2C12 myoblasts. Magnification, ×20. (**B**) Western blot analysis of BGN in cytosol and nuclear fractions of C2C12 myoblasts. $n = 3$. (**C**) Immunofluorescence staining of CLIC5 and BGN in C2C12 myoblasts. Magnification, ×40. (**D**) Reciprocal coimmunoprecipitation (IP) analysis between Flag-tagged CLIC5 and Myc-tagged BGN in HEK293T cells. IB, immunoblotting. (**E**) CLIC5/BGN binding domain identification. Full-length and C-terminal truncated CLIC5 were overexpressed with HA-tagged BGN in HEK293T cells. Immunoblot for HA after anti–green fluorescent protein (GFP) coimmunoprecipitation. (**F**) Immunofluorescence staining of BGN in WT and CLIC5-KO C2C12 myoblasts. Magnification, ×60. (**G** to **H**) Western blot analysis of BGN in cytosol and plasma membrane (PM) fractions of WT and KO C2C12 myoblasts. (**I**) Western blot analysis of BGN after CLIC5 overexpression in C2C12 myoblasts. The data present means ± SEM ($n = 3$). $^{**}P < 0.01$.

the significant increase in embryonic myosin heavy chain-positive ($eMyHC^+$) myofibers observed at day 3 after injury with CLIC5 overexpression (Fig. 7C). In addition, at this stage, significant enhancement was observed in the expression levels of Pax7, BGN, active β-catenin, Axin2, GSK-3β, and CK1α in TA muscle treated with AAV9:CLIC5 compared to those administered AAV9:empty vector, corresponding to the increased CLIC5 protein levels (Fig. 7, D and E). At day 3 after injury, CLIC5 overexpression increased expression levels of Pax7, BGN, axin2, and GSK-3β (fig. S9, A and B) and Wnt target genes (*Nphs1* and *Cdc25c*; fig. S9C) in MuSCs. This suggests that CLIC5 overexpression in skeletal muscle enhances muscle regeneration through the BGN-mediated canonical Wnt/β-catenin signaling pathway.

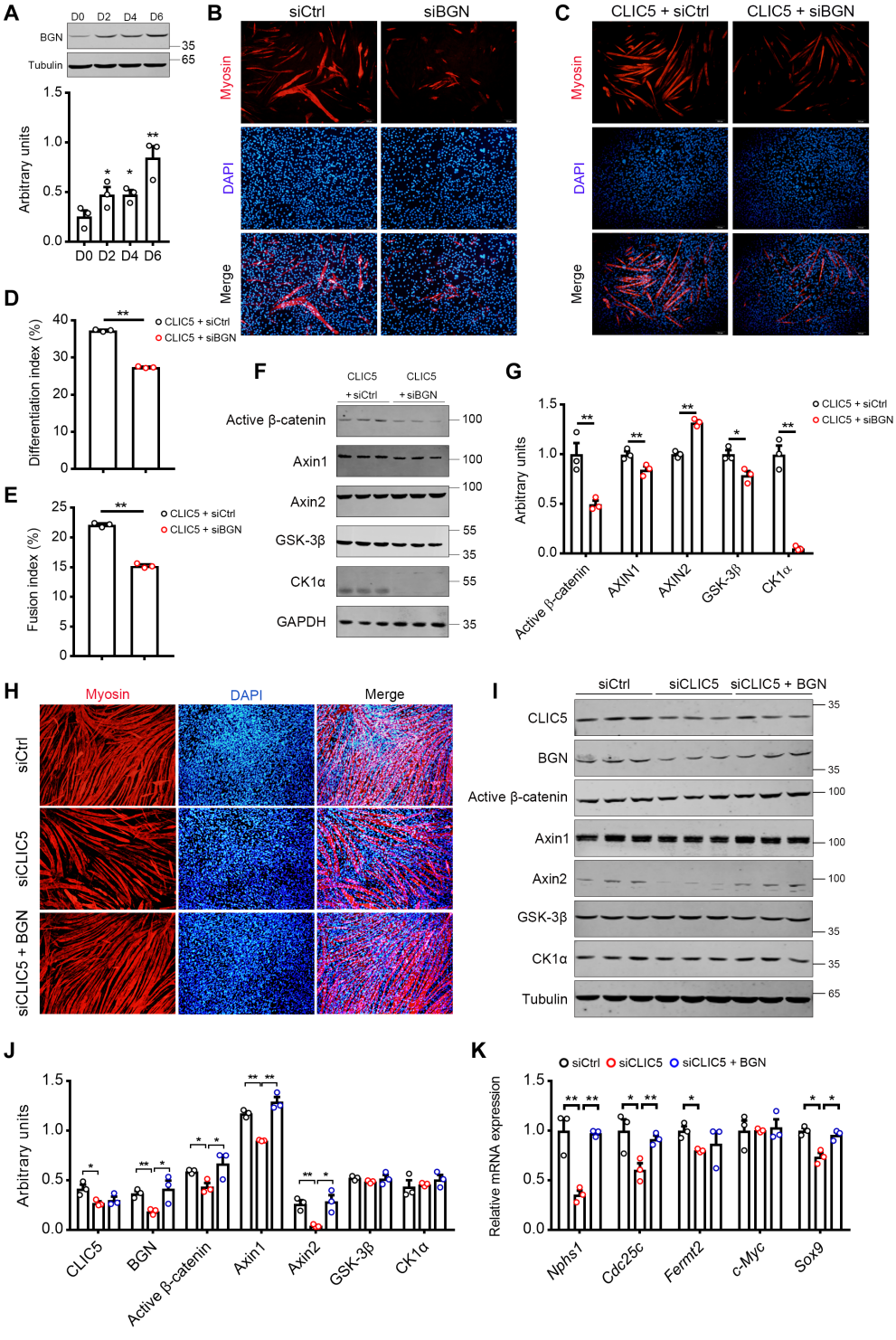


**Fig. 5. CLIC5 promotes myoblast differentiation and activates canonical Wnt/β-catenin signaling pathway through BGN.** (**A**) Western blot analysis of BGN in C2C12 myoblasts cultured in growth medium (D0) or in DM for 2, 4, or 6 days. Immunofluorescence analysis for myosin in siCtrl and siBGN C2C12 myoblasts (**B**) or myoblasts stably transfected with CLIC5 plasmid (**C**) after 4 days in DM. Magnification, ×10. (**D**) Differentiation index. (**E**) Fusion index. (**F** and **G**) Western blot analysis of active β-catenin, Axin1, Axin2, GSK-3β, and CK1α in siCtrl and siBGN C2C12 myoblasts stably transfected with CLIC5 plasmid. Immunofluorescence analysis for myosin (**H**), Western blot analysis of CLIC5, BGN, and canonical Wnt/β-catenin signaling pathway (**I** and **J**), as well as relative mRNA levels of Wnt-targeted genes (**K**) in siCtrl, siCLIC5, and siCLIC5 C2C12 myoblasts transfected with BGN plasmid after 6 days in DM. Magnification, ×10. The data present means ± SEM ($n = 3$). *$P < 0.05$ and **$P < 0.01$.

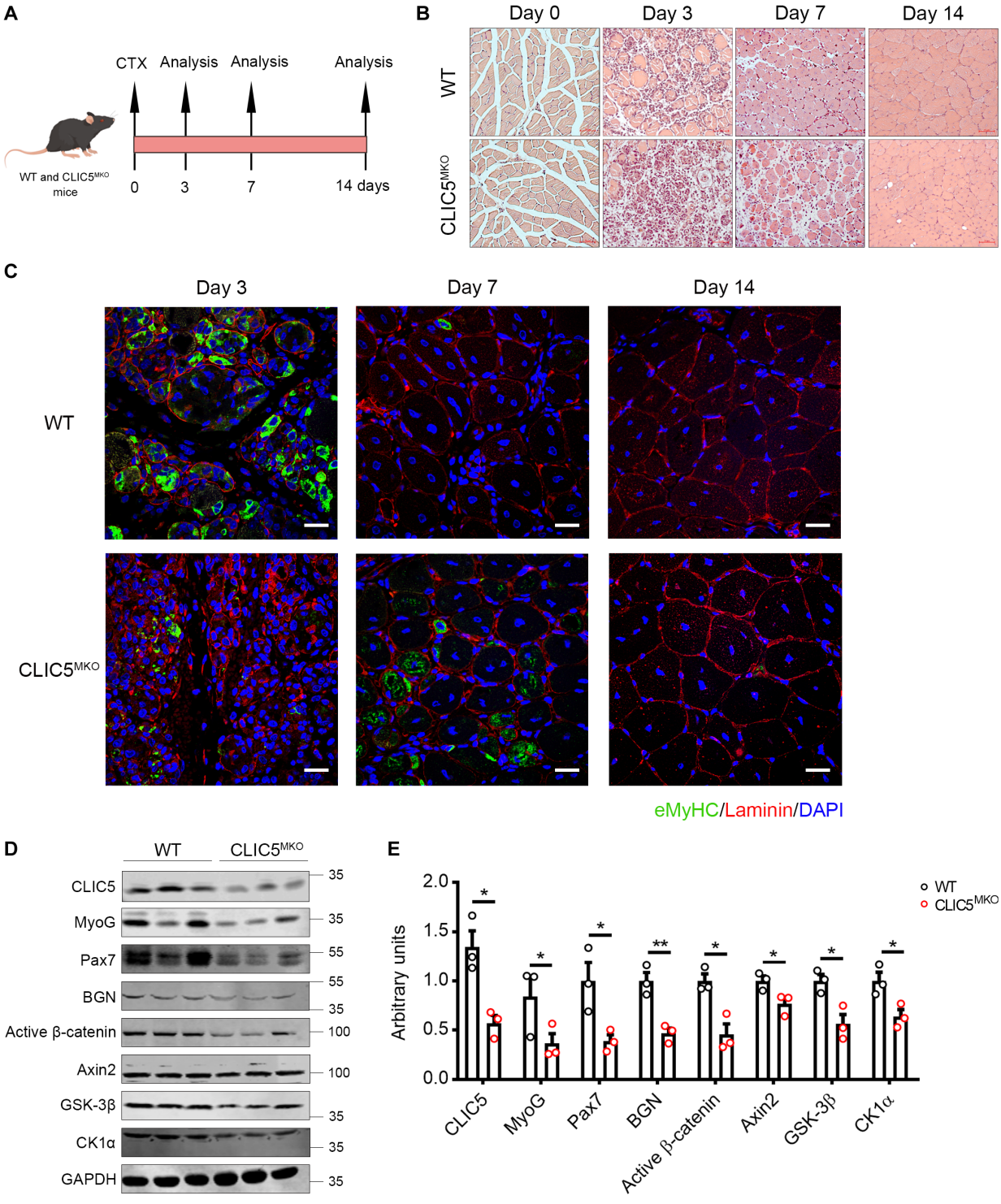


**Fig. 6. Loss of CLIC5 impairs skeletal muscle regeneration.** (**A**) Schematic outline of cardiotoxin (CTX) injection and sample collection. (**B**) Hematoxylin and eosin (H&E) staining of injured TA muscle in WT and CLIC5$^{MKO}$ mice at days 0, 3, 7 and 14 after injury. Magnification, ×20. (**C**) Immunofluorescence analysis of eMyHC$^{+}$ fibers in TA muscles at days 3, 7, and 14 after injury. Scale bar, 50 μm. (**D** and **E**) Western blot analysis of CLIC5, MyoG, Pax7, BGN, active β-catenin, Axin2, GSK-3β, and CK1α in the TA muscle of WT and CLIC5$^{MKO}$ mice at day 3 after injury. The data present means ± SEM ($n = 3$). *$P < 0.05$ and **$P < 0.01$.

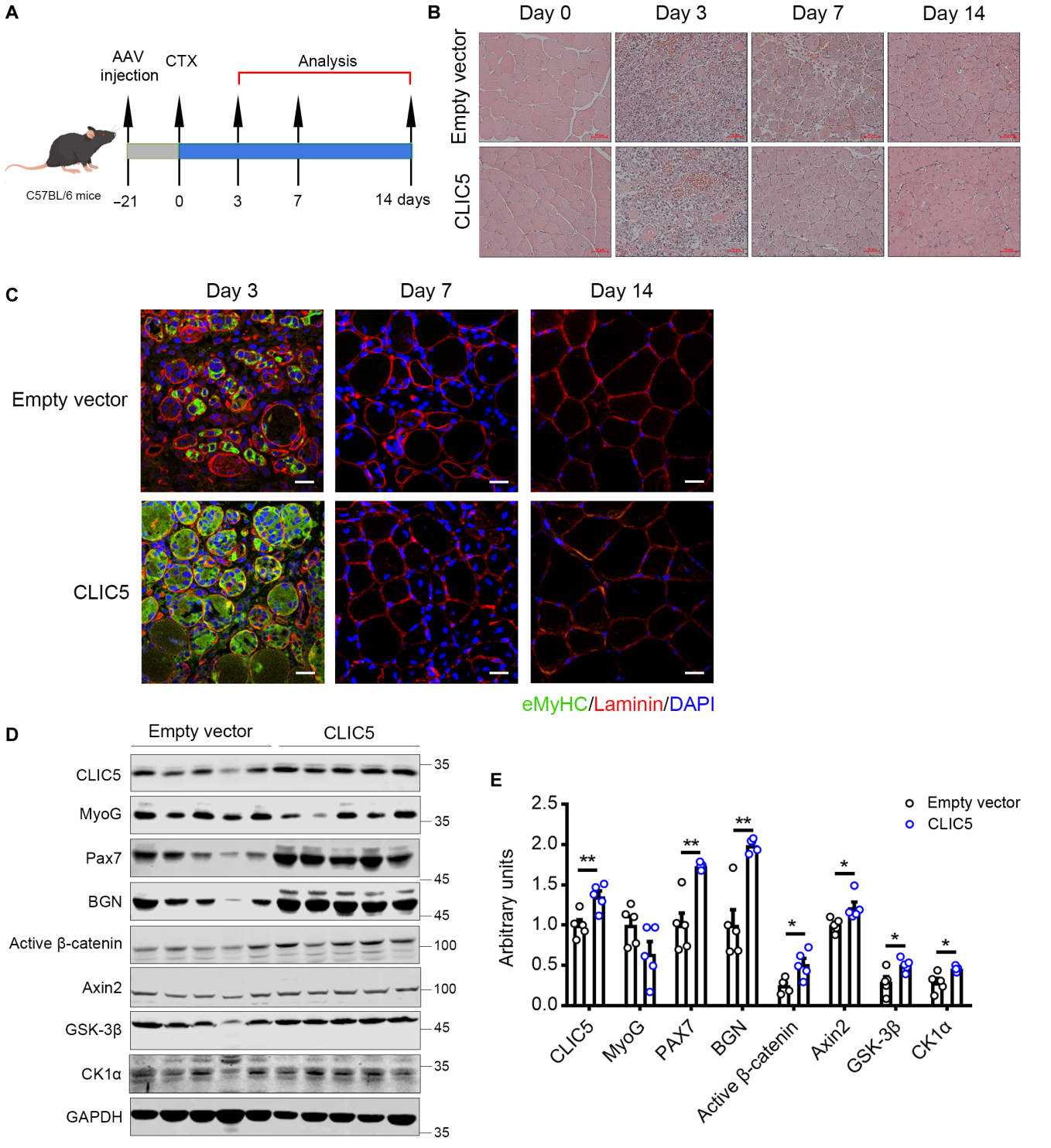


**Fig. 7. Increasing CLIC5 in the skeletal muscle enhances its regeneration capacity.** (**A**) Schematic outline of the administration of AAV9:empty vector or AAV9:CLIC5 vectors, CTX injection, and sample collection. (**B**) H&E staining of injured TA muscle at days 0, 3, 7, and 14 after injury. Magnification, ×20. (**C**) Immunofluorescence analysis of eMyHC$^{+}$ fibers in TA muscles at days 3, 7, and 14 after injury. Scale bar, 50 μm. (**D** and **E**) Western blot analysis of CLIC5, MyoG, Pax7, BGN, active β-catenin, Axin2, GSK-3β, and CK1α in the TA muscle of mice administered AAV9:empty vector or AAV9:CLIC5 vectors at day 3 after injury. The data present means ± SEM ($n = 5$). *$P < 0.05$ and **$P < 0.01$.

## DISCUSSION

Skeletal muscle, the largest tissue in humans, is crucial for movement and overall systemic health (*23*). Substantial loss of muscle mass and function presents a major quality-of-life challenge, particularly among older individuals. Extensive research has focused on muscle regeneration after injury, aiming to develop effective therapies for restoring optimal muscle structure and function in cases where regeneration is impaired (*1*). While noncoding RNAs, such as long noncoding RNA and circular RNA, have been extensively studied in muscle regeneration (*24*, *25*), the precise role of protein-coding genes, which form the core of the networks controlling myogenesis and muscle regeneration, remains incompletely understood.

The study conducted in MuSCs and myoblasts confirmed that CLIC5 promotes myogenic differentiation by activating the canonical Wnt/β-catenin signaling pathway. Myoblasts without β-catenin experience delayed differentiation, while those constitutively active β-catenin undergo premature differentiation, highlighting the importance of precise β-catenin levels in regulating myoblast proliferation and differentiation (*26*). In the absence of Wnt ligands, β-catenin is phosphorylated by a cytoplasmic destruction complex, ubiquitinated, and then destructed by the proteasome. However, in this study, protein levels of both active β-catenin and destruction complex were decreased or increased in CLIC5-KO or -overexpressing myoblasts, suggesting that CLIC5 may promote the recruitment of destruction complex but block the degradation of β-catenin.

Mechanistically, CLIC5 interacts with BGN to activate canonical Wnt/β-catenin signaling. BGN, a member of the small, leucine-rich proteoglycan family, plays an important role in bone homeostasis and development. BGN-deficient mice exhibited bone formation defects and age-related osteopenia (*27*). Notably, overexpression of human BGN ameliorated motor deficits and improved myofiber size of mdx mice (*28*). In our study, CLIC5 enhances BGN expression, and CLIC5-promoted myoblast differentiation almost vanishes after BGN knockdown, suggesting that CLIC5 promotes myoblast differentiation through BGN. We found that BGN binds with CLIC5 domain consisting of residues 1 to 105. A recent study revealed that CLIC5 served as a fusogen, with F34 (phenylalanine 34 residue) playing a crucial role (*29*). However, the role of CLIC5 in myoblast fusion remains unclear. F34 is highly conserved across CLICs; its mutation in CLIC4 prevented its translocation to the cell membrane (*30*). Therefore, the role of this phenylalanine residue in the binding of CLIC5 and BGN also needs to be elucidated.

The correlation of BGN with Wnt signaling has also been shown in the skeletal system (*22*, *31*). BGN directly interacts with Wnt3a, and in calvarial cells lacking BGN, Wnt3a-induced Axin2 expression and β-catenin translocation were reduced (*22*), similar to the effect of CLIC5 on Wnt/β-catenin signaling. In addition, BGN knockdown inhibits CLIC5-activated Wnt/β-catenin signaling, suggesting that CLIC5 enhances canonical Wnt/β-catenin signaling through BGN. This study enhances our knowledge of regulators that affect canonical Wnt/β-catenin signaling in myogenesis and muscle regeneration.

Apart from the canonical Wnt/β-catenin signaling, RNA-seq analysis of control and CLIC5-KO myoblasts reveals significant alterations in the Hippo signaling pathway. This pathway is crucial in regulating organ development by controlling the activity of transcriptional coactivators Yap and Taz (*32*, *33*). C2C12 myoblasts with stable YAP expression exhibited improved myotube formation (*34*), while mice treated with Yap–short hairpin RNA consistently exhibited reduced lean mass and body mass due to smaller muscle fiber size (*35*). Kyoto Encyclopedia of Genes and Genomes analysis also reveals a strong connection between CLIC5 and ubiquitin-mediated proteolysis. The ubiquitin-proteasome system is responsible for removing aggregated and dysfunctional proteins, crucial for maintaining skeletal muscle mass and function (*36*). These findings further underscore the significance of CLIC5 in myogenesis. Note that there are some apparent discrepancies between the in vivo and in vitro findings. Briefly, loss of CLIC5 reduced the self-renewal of MuSCs but promoted the proliferation of C2C12 myoblasts. Myotube formation is absent in CLIC5-KO C2C12 myoblasts, but CLIC5 conditional KO in skeletal muscle delays but not blocks MuSC differentiation. C2C12 is an established immortal cell line derived from MuSCs of C3H mouse. Differences in the properties of C2C12 myoblasts and MuSCs have been reported in the previous study (*37*), which may lead to the inconsistent influence of CLIC5 on cell proliferation in vivo and in vitro. Myogenic differentiation of MuSCs is influenced by signaling from surrounding cells, such as fibroadipogenic progenitors and macrophage (*38*–*40*). The effect of CLIC5 on MuSC differentiation may be also influenced by the local milieu. Anyway, studies conducted in C2C12 myoblasts and MuSCs strongly demonstrate that CLIC5 promotes myogenic differentiation.

In accordance with the absolute requirement for myogenic differentiation in skeletal muscle hypertrophy and regeneration (*3*, *41*), muscle growth and regeneration are impaired in vivo following CLIC5-specific deletion in Myf5-expressing embryonic committed myogenic cells and their descendant MuSCs and myofibers. Noteworthy, our study reveals that CLIC5 deficiency in vivo reduces the activity of the BGN-mediated canonical Wnt/β-catenin signaling pathway and decreases the protein level of Pax7 at day 3 after injury, consistent with our observations in MuSCs. Pax7 acts as a nodal factor in stimulating proliferation and inhibiting differentiation of MuSCs (*42*, *43*). Conditional loss of Pax7 in adult mice strongly impaired muscle generation due to proliferation defects and precocious differentiation of MuSCs (*44*, *45*). The transition from high Notch to high Wnt activation is essential for efficient muscle repair and regeneration (*10*). There was a significant increase in canonical Wnt signaling at days 2 and 5 after injury within regenerating muscle (*10*). Pax7 is downstream of Wnt/β-catenin signaling during myoblast differentiation. Consequently, our study strongly indicates that the combined decrease in $Pax7^{+}$ MuSCs, Pax7 levels, and the Wnt/β-catenin signaling pathway contributes significantly to the delayed skeletal muscle regeneration. In addition, although the muscle fully regenerated by day 14 in $CLIC5^{MKO}$ mice, CLIC5 KO reduced the Pax7 levels and the pool of MuSCs. This suggests that the muscle regeneration in $CLIC5^{MKO}$ mice may be at the expense of MuSC self-renewal, which could lead to regenerative defects during aging, as reported in the previous study (*41*). As shown in Fig. 6C, increased eMyHC expression was detected at day 7 after injury in $CLIC5^{MKO}$ mice, which may indicate compensatory activation in MuSCs to support muscle regeneration. Of course, CLIC5 protein levels were reduced by 57.7% in TA muscle and 87.5% in MuSCs in $CLIC5^{MKO}$ mice. Therefore, a small proportion of MuSCs are escapers of CLIC5 deletion. These escapers and nonmyogenic lineages within skeletal muscle may contribute to the rescue of muscle

regeneration defects in CLIC5$^{MKO}$ mice, which warrants further investigation. Conversely, overexpressing CLIC5 in the TA muscle significantly increases Pax7 and BGN protein levels, along with activating the canonical Wnt/β-catenin signaling. This overexpression also shows positive effects on skeletal muscle regeneration. This study identifies CLIC5 as a potential target for enhancing skeletal muscle regeneration capacity.

Some limitations of this study should be noted. Although the binding of CLIC5 and BGN has been demonstrated in this study, the exact binding site of CLIC5 and BGN remains unclear. To fully understand the role of CLIC5 in skeletal muscle development, the effects of CLIC5 KO on embryonic myogenesis and key signaling within the dermomyotome warrant future investigation. From a mechanistic perspective, we show that CLIC5 is essential for maintaining the MuSC pool, but the shrinking MuSC pool size may be due to the defects in embryonic myoblasts or the direct influence of CLIC5 on MuSCs. To address this concern, conditional deletion of CLIC5 in MuSCs of adult skeletal muscles using Pax7-CreER mice should be performed.

In conclusion, our studies demonstrate that CLIC5 is a key determinant in maintaining MuSCs pool and regulating the proliferation and differentiation of myoblasts. CLIC5 promotes myogenic differentiation by activating the canonical Wnt/β-catenin signaling pathway in a BGN-dependent manner. Importantly, CLIC5 deficiency in skeletal muscles leads to impaired muscle regeneration due to a substantial decline in MuSCs function. Our findings establish CLIC5 as a pivotal regulator of skeletal muscle regeneration, suggesting that interventions targeting CLIC5 could enhance muscle regeneration and function.

## MATERIALS AND METHODS

### Ethics statement

All mouse experimental procedures and protocols were performed strictly in accordance with the guidelines of the Beijing Laboratory Animal Management and were authorized by the Institutional Animal Care and Use Committee of China Agricultural University (approval number: SKLAB2019-04-03).

### CLIC5 conditional KO mice

*CLIC5*$^{fl/fl}$ mice were generated using CRISPR-Cas9 genome-editing system and facilitated by Cyagen Biosciences (Guangzhou, China). For the generation of *CLIC5*$^{fl/fl}$ mice, targeting vector was constructed by inserting a flippase recombination target (Frt)-flanked neomycin cassette upstream and two loxP sites downstream of the second exon of *CLIC5* and then electroporated into embryonic stem cells from C57BL/6 mice. Skeletal muscle–conditional CLIC5-KO mice were generated by crossbreeding of *CLIC5*$^{fl/fl}$ mice with Myf5-Cre mice (J007893, from the Jackson Laboratory). The genotype was determined by PCR from tail DNA using the primers in table S3. Mice were kept in a temperature-controlled environment (23° ± 2°C) and free access to food and water under a 12-hour/12-hour light/dark cycle.

### Generation of serotype 9 recombinant AAV vectors and their intramuscular injections

Mouse CLIC5 transcripts were synthesized and subcloned into AAV9:CMV-MSC-3×Flag-EF1-ZsGreen-T2A-Puro plasmids by Hanbio Technology (Shanghai, China). Eight-week-old male C57BL/6J mice were administered intramuscular injection of AAV9 vectors. Mice were anesthetized before receiving TA injections of either empty vectors (AAV9:CMV-MSC-3×Flag-EF1-ZsGreen-T2A-Puro) or AAV9 vectors encoding mouse CLIC5 diluted in 40 μl of Hanks' balanced salt solution to a dosage of $1 \times 10^{12}$ vg. Three weeks after injection, mice were used to induce TA injury.

### Skeletal muscle injury

Fifty microliters of CTX (10 μM; 217503, Sigma-Aldrich, USA) was injected into hindlimb TA muscles. The TA muscles were harvested at days 3, 7, and 14 after injury and fixed with 4% paraformaldehyde for histological analysis or immunofluorescence. At least three mice were analyzed for each time point after CTX injection.

### Culture and maintenance of cells

C2C12 myoblasts and HEK293T cell lines were purchased from the American Type Culture Collection (USA). The two cell lines were cultured in growth medium containing 10% fetal bovine serum (FBS; Gibco, USA) in Dulbecco's modified Eagle's medium (DMEM; high glucose; Gibco, USA).

MuSCs were isolated from the skeletal muscle of 8-week-old CLIC5$^{MKO}$ mice or CLIC5-overexpressing mice at day 3 after injury as described previously (*46*). Briefly, the hindlimb muscles were minced and digested with 0.2% type II collagenase (11088815001, Roche, Switzerland) and dispase (2.5 U/ml; D4693, Sigma-Aldrich, USA) for 1 hour. Each sample was consecutively filtered through 70- and 40-μm cell strainers. The cell suspension was then centrifuged at 1000*g*. Last, the pellet was washed with FACS buffer [5% FBS and 1% PS in phosphate-buffered saline (PBS)] and stained with CD31–fluorescein isothiocyanate (FITC), CD45-FITC, Sca1-PerCP, and $\alpha_7$ integrin–AF700 for 1 hour at 4°C. Information of antibodies was listed in table S4. MuSCs were sorted with the characteristics of CD31$^-$, CD45$^-$, Sca1$^-$, and $\alpha_7$ integrin$^+$ cells. FACS-purified MuSCs were cultured in six-well plates in DMEM supplemented with 20% FBS, antibiotics [penicillin (100 U/ml) and streptomycin (100 mg/ml)] and basic fibroblast growth factor (5 ng/ml; Proteintech, USA). To verify the role of canonical Wnt signaling, C2C12 myoblasts or MuSCs were treated with BML-284 (10 μM; HY-29987, MedChemExpress, USA) or dimethyl sulfoxide in DM.

### Myogenic differentiation

For myogenic induction, C2C12 myoblasts or MuSCs at 80 to 90% confluence were switched to myogenic DM consisting of 2% horse serum in DMEM (high glucose). Myogenic differentiation was characterized by the formation of myosin-positive multinucleated myotubes. The differentiation and fusion indices were calculated as the percentage of nuclei within myosin-positive cells and myosin-positive myotubes, respectively (*47*). Structures containing at least two nuclei were considered myotubes.

### Cell proliferation assay

Cells were seeded in 96-well plates at a density of $5 \times 10^3$ cells. Upon reaching 70 to 80% confluence, the cells were incubated with EdU for 2 hours before staining. Cell proliferation was assessed using the Cell-Light EdU Cell Proliferation Detection Kit (C10310, RiboBio, China) following the instructions of the manufacturer. The percentage of proliferating cells was calculated by quantifying the EdU-positive cells under a fluorescence microscope (CK40, Olympus, Japan).

For cell cycle analysis, cells at 70 to 80% confluence were trypsinized and fixed overnight with 75% ethanol at −20°C. Subsequently, they were treated with propidium iodide (50 g/ml; P8080, Beijing Solarbio Science & Technology Co. Ltd., China) for 30 min at 37°C in the dark. A total of 10,000 cells were counted per sample, and cell cycle phase was measured by propidium iodide staining intensity using a flow cytometer (BD Biosciences). The data generated were analyzed using FlowJo 10 software (FlowJo LLC, USA) to determine the proportion of each cell cycle.

### RNA interference

C2C12 myoblasts at 70 to 80% confluence were transfected with 100 nM siRNA (Ribobio, China) using Lipofectamine 3000 (L3000, Invitrogen, USA) according to the manufacturer's protocol. After 48 hours of transfection, cells were collected or induced for myogenic differentiation. The sequences of siRNA used in this study were listed in table S5.

### Construction and packing of lentivirus

For stable gene expression in C2C12 myoblasts, the *CLIC5* gene was cloned into pHBLV-puro vector with Flag tags. Recombinant lentiviruses were produced by cotransfecting HEK293T cells with the lentiviral expression and packaging plasmids psPAX2 and pMD2.G, respectively. Medium containing virus was harvested at 48 and 72 hours after cell transfection, and the virus was filtered through a 0.45-μm filter before infection.

### Plasmid construction and transfection

The plasmid encoding CLIC5-Flag was created by adding a Flag tag to the C terminus of CLIC5, which was then cloned into the Bam HI and Eco RI sites of the pcDNA3.1(+) vector (Invitrogen). A plasmid encoding BGN-Myc was created by adding a Myc tag to the C terminus of BGN, followed by cloning it into Bam HI and Eco RI sites of the pcDNA3.1(+) vector (Invitrogen, USA). The resulting BGN-Myc plasmids, along with the CLIC5-Flag plasmid, were transfected into HEK293T cells using Lipofectamine 3000 (L3000, Invitrogen, USA). Samples were collected 24 hours after transfection.

### Construction of CLIC5-KO C2C12 myoblasts

Four single guide RNA sequences were designed and synthesized on the basis of CLIC5 gene information. These sequences were cloned into the pSpCas9 (BB)–2A–puro (px458) plasmid. The activities of these single guide RNAs were analyzed using the T7E1 assay, and those with the highest activity were selected for subsequent experiments. To create a CLIC5-KO C2C12 myoblasts, px458-sgCLIC5 was transfected into C2C12 myoblasts using Lipofectamine 3000 (L3000, Invitrogen, USA). After transfection for 2 days, single cell–derived clone was sorted via puromycin (5 μg/ml) treating. Following 7 to 10 days of expansion, the clones underwent screening for CRISPR-mediated deletions using Sanger sequencing.

### Subcellular fractionation

For nuclear and cytosolic extraction, C2C12 myoblasts were harvested, and subcellular fractionation was performed with a NE-PER nuclear and cytoplasmic extraction kit (78835, Thermo Fisher Scientific, USA) according to the manufacturer's protocol. Membrane proteins were extracted using the Mem-PER Plus Membrane Protein Extraction Kit (89842, Thermo Fisher Scientific, USA) according to the manufacturer's instruction. Supernatant-containing cytosolic proteins were obtained after permeabilization and centrifugation during membrane proteins extraction.

### RNA isolation and qPCR

Total RNA was isolated from frozen muscles or C2C12 myoblasts using the HiPure Total RNA Mini Kit (R4130, Magen, China). The RNA was reverse transcribed into cDNA using the PrimeScript RT Reagent Kit with gDNA Eraser (RR047A, Takara, Japan) following the protocol of the manufacturer. SYBR Green–based qPCR was performed in a qTOWER 2.2 thermocycler (Analytik Jena, German). The mRNA expression levels of target genes were normalized to that of *GAPDH*. The primer sequences for qPCR were listed in table S6.

### Identification of CLIC5 interacting partners by mass spectrometry analysis

Immunoprecipitation was conducted using the Immunoprecipitation Kit (PK10007, Proteintech, USA) according to the manufacturer's instructions. Briefly, C2C12 myoblasts were lysed in lysis buffer for 30 min. Antibody against CLIC5, coupled to sepharose beads, was incubated with cell lysate overnight at 4°C. The bound proteins were resolved by SDS–polyacrylamide gel electrophoresis and visualized by Coomassie blue staining. The gel lanes were excised and cut from top to bottom into small pieces and subjected to mass spectrometry analysis (EASY-nLC 1000 System, Thermo Fisher Scientific).

### Western blot analysis and immunoprecipitation analysis

Cell samples and TA tissues were lysed in radioimmunoprecipitation assay lysis buffer (Huaxingbio, China) with protease inhibitor cocktail (Roche, Switzerland). Approximately 40 to 80 μg of total protein was resolved on 8 to 12% SDS–polyacrylamide gel electrophoresis gels and transferred to polyvinylidene fluoride membranes (Millipore, USA). Membrane was blocked in tris-buffered saline containing 5% (w/v) skimmed milk powder or bovine serum albumin at room temperature for 1 hour and then incubated against corresponding primary antibodies at 4°C overnight. After washing with TBST, blots were developed using DyLight 800–labeled secondary antibodies, detected by the Odyssey Clx (LI-COR Biotechnology, USA), and quantified by ImageJ software (National Institutes of Health, USA). HEK293T cells, which were transfected with CLIC5-Flag or BGN-Myc plasmids, were used for immunoprecipitation analysis by the Immunoprecipitation Kit (PK10007, Proteintech, USA). Cells were lysed with immunoprecipitation lysis buffer, and the total protein was immunoprecipitated with Flag or Myc antibody and sepharose beads. Immunocomplexes were washed three times with immunoprecipitation lysis buffer and analyzed by Western blot. The information of primary and secondary antibodies was listed in table S4.

### Histological analysis

TA muscles were collected, fixed in 4% paraformaldehyde, and underwent paraffin histology processing. Paraffin-embedded samples were sectioned into 5-μm-thick transverse sections, followed by staining with H&E.

### Immunofluorescence

Muscle sections and cultured cells were fixed with 4% paraformaldehyde, permeabilized with 0.2% Triton X-100 for 10 min, blocked in blocking solution containing 5% bovine serum albumin in PBS

for 1.5 hours, and incubated with primary antibodies overnight at 4°C. Subsequently, the samples were washed three times with PBS and stained with secondary antibody conjugated to Alexa Fluor 594 or Alexa Fluor 488 for 1 hour at room temperature. Following washing with PBS, cells were incubated with 4ells were incubated with ted (DAPI) (C0060, Beijing Solarbio Science & Technology Co. Ltd., China) for 10 min to stain nuclei. Fluorescence was visualized using fluorescence microscope (CK40, Olympus, Japan) or confocal laser scanning microscopy (LSM800, Zeiss, Germany). The primary antibodies used for immunofluorescence were listed in table S4.

### RNA sequencing

Total RNAs were extracted from cultured WT and CLIC5-KO C2C12 myoblasts using the HiPure Total RNA Mini Kit with DNA filter (R4111, Magen, China). After evaluating the quantity and quality of RNA using a NanoDrop spectrophotometer (Thermo Fisher Scientific, USA), sequencing libraries were constructed with the NEB Next Ultra Directional RNA Library Prep Kit for Illumina (E7760, NEB, USA) according to the manufacturer's recommendations. The number of reads mapped to each gene was counted by HRSeq v0.5.3. Reads per kilobases per million reads were applied to quantify gene expression. R package DESeq2 (v1.4.5) was used to figure out the DEGs between WT and CLIC5-KO C2C12 myoblasts.

### Statistical analysis

All experiments included at least three biological replicates. Normal distribution of populations at the 0.05 level was calculated using Kolmogorov-Smirnov test. Statistical differences were determined by the unpaired two-tailed Student's *t* test procedures of SAS (v.9.2, SAS Institute, USA). A value of $P < 0.05$ was considered significant.

## Supplementary Materials

**This PDF file includes:**

Figs. S1 to S9
Tables S1 to S6
Uncropped Western blots

## REFERENCES AND NOTES


1. M. N. Wosczyna, T. A. Rando, A muscle stem cell support group: Coordinated cellular responses in muscle regeneration. *Dev. Cell* **46**, 135–143 (2018).
2. I. Janssen, S. B. Heymsfield, Z. M. Wang, R. Ross, Skeletal muscle mass and distribution in 468 men and women aged 18–88 yr. *J. Appl. Physiol.* **89**, 81–88 (2000).
3. H. Yin, F. Price, M. A. Rudnicki, Satellite cells and the muscle stem cell niche. *Physiol. Rev.* **93**, 23–67 (2013).
4. S. B. Chargé, M. A. Rudnicki, Cellular and molecular regulation of muscle regeneration. *Physiol. Rev.* **84**, 209–238 (2004).
5. N. Zanou, P. Gailly, Skeletal muscle hypertrophy and regeneration: Interplay between the myogenic regulatory factors (MRFs) and insulin-like growth factors (IGFs) pathways. *Cell. Mol. Life Sci.* **70**, 4117–4130 (2013).
6. F. Le Grand, A. E. Jones, V. Seale, A. Scimè, M. A. Rudnicki, Wnt7a activates the planar cell polarity pathway to drive the symmetric expansion of satellite stem cells. *Cell Stem Cell* **4**, 535–547 (2009).
7. W. Pan, Y. Jia, J. Wang, D. Tao, X. Gan, L. Tsiokas, N. Jing, D. Wu, L. Li, Beta-catenin regulates myogenesis by relieving I-mfa-mediated suppression of myogenic regulatory factors in P19 cells. *Proc. Natl. Acad. Sci. U.S.A.* **102**, 17378–17383 (2005).
8. S. Cui, L. Li, R. T. Yu, M. Downes, R. M. Evans, J. A. Hulin, H. P. Makarenkova, R. Meech, β-Catenin is essential for differentiation of primary myoblasts via cooperation with MyoD and α-catenin. *Development* **146**, dev167080 (2019).
9. G. Cossu, U. Borello, Wnt signaling and the activation of myogenesis in mammals. *EMBO J.* **18**, 6867–6872 (1999).
10. A. S. Brack, I. M. Conboy, M. J. Conboy, J. Shen, T. A. Rando, A temporal switch from Notch to Wnt signaling in muscle stem cells is necessary for normal adult myogenesis. *Cell Stem Cell* **2**, 50–59 (2008).
11. A. Suzuki, R. C. Pelikan, J. Iwata, Wnt/β-catenin signaling regulates multiple steps of myogenesis by regulating step-specific targets. *Mol. Cell. Biol.* **35**, 1763–1776 (2015).
12. A. Parisi, F. Lacour, L. Giordani, S. Colnot, P. Maire, F. Le Grand, APC is required for muscle stem cell proliferation and skeletal muscle tissue repair. *J. Cell Biol.* **210**, 717–726 (2015).
13. J. von Maltzahn, N. C. Chang, C. F. Bentzinger, M. A. Rudnicki, Wnt signaling in myogenesis. *Trends Cell Biol.* **22**, 602–609 (2012).
14. Z. K. Zhang, J. Li, D. Guan, C. Liang, Z. Zhuo, J. Liu, A. Lu, G. Zhang, B. T. Zhang, A newly identified lncRNA MAR1 acts as a miR-487b sponge to promote skeletal muscle differentiation and regeneration. *J. Cachexia. Sarcopenia Muscle* **9**, 613–626 (2018).
15. F. Lacour, E. Vezin, C. F. Bentzinger, M. C. Sincennes, L. Giordani, A. Ferry, R. Mitchell, K. Patel, M. A. Rudnicki, M. C. Chaboissier, A. A. Chassot, F. Le Grand, R-spondin1 controls muscle cell fusion through dual regulation of antagonistic Wnt signaling pathways. *Cell Rep.* **18**, 2320–2330 (2017).
16. L. H. Gagnon, C. M. Longo-Guess, M. Berryman, J. B. Shin, K. W. Saylor, H. Yu, P. G. Gillespie, K. R. Johnson, The chloride intracellular channel protein CLIC5 is expressed at high levels in hair cell stereocilia and is essential for normal inner ear function. *J. Neurosci.* **26**, 10188–10198 (2006).
17. E. M. Bradford, M. L. Miller, V. Prasad, M. L. Nieman, L. R. Gawenis, M. Berryman, J. N. Lorenz, P. Tso, G. E. Shull, CLIC5 mutant mice are resistant to diet-induced obesity and exhibit gastric hemorrhaging and increased susceptibility to torpor. *Am. J. Physiol. Regul. Integr. Comp. Physiol.* **298**, R1531–R1542 (2010).
18. F. N. Li, J. D. Yin, J. J. Ni, L. Liu, H. Y. Zhang, M. Du, Chloride intracellular channel 5 modulates adipocyte accumulation in skeletal muscle by inhibiting preadipocyte differentiation. *J. Cell. Biochem.* **110**, 1013–1021 (2010).
19. F. Li, J. Yin, T. Yue, L. Liu, H. Zhang, The CLIC5 (chloride intracellular channel 5) involved in C2C12 myoblasts proliferation and differentiation. *Cell Biol. Int.* **34**, 379–384 (2010).
20. L. Ji, B. Lu, R. Zamponi, O. Charlat, R. Aversa, Z. Yang, F. Sigoillot, X. Zhu, T. Hu, J. S. Reece-Hoyes, C. Russ, G. Michaud, J. S. Tchorz, X. Jiang, F. Cong, USP7 inhibits Wnt/β-catenin signaling through promoting stabilization of Axin. *Nat. Commun.* **10**, 4184 (2019).
21. B. Chen, W. You, T. Shan, Myomaker, and Myomixer-Myomerger-Minion modulate the efficiency of skeletal muscle development with melatonin supplementation through Wnt/β-catenin pathway. *Exp. Cell Res.* **385**, 111705 (2019).
22. A. D. Berendsen, L. W. Fisher, T. M. Kilts, R. T. Owens, P. G. Robey, J. S. Gutkind, M. F. Young, Modulation of canonical Wnt signaling by the extracellular matrix component biglycan. *Proc. Natl. Acad. Sci. U.S.A.* **108**, 17022–17027 (2011).
23. W. J. Evans, J. Guralnik, P. Cawthon, J. Appleby, F. Landi, L. Clarke, B. Vellas, L. Ferrucci, R. Roubenoff, Sarcopenia: No consensus, no diagnostic criteria, and no approved indication-How did we get here? *Geroscience* **46**, 183–190 (2024).
24. J. J. Jin, W. Lv, P. Xia, Z. Y. Xu, A. D. Zheng, X. J. Wang, S. S. Wang, R. Zeng, H. M. Luo, G. L. Li, B. Zuo, Long noncoding RNA *SYISL* regulates myogenesis by interacting with polycomb repressive complex 2. *Proc. Natl. Acad. Sci. U.S.A.* **115**, E9802–E9811 (2018).
25. K. Huang, Z. Li, D. Zhong, Y. Yang, X. Yan, T. Feng, X. Wang, L. Zhang, X. Shen, M. Chen, X. Luo, K. Cui, J. Huang, S. U. Rehman, Y. Jiang, D. Shi, A. Pauciullo, X. Tang, Q. Liu, H. Li, A circular RNA generated from Nebulin (NEB) gene splicing promotes skeletal muscle myogenesis in cattle as detected by a multi-omics approach. *Adv. Sci.* **11**, e2300702 (2024).
26. A. Rudolf, E. Schirwis, L. Giordani, A. Parisi, C. Lepper, M. M. Taketo, F. Le, Grand, β-catenin activation in muscle progenitor cells regulates tissue repair. *Cell Rep.* **15**, 1277–1290 (2016).
27. T. Xu, P. Bianco, L. W. Fisher, G. Longenecker, E. Smith, S. Goldstein, J. Bonadio, A. Boskey, A. M. Heegaard, B. Sommer, K. Satomura, P. Dominguez, C. Zhao, A. B. Kulkarni, P. G. Robey, M. F. Young, Targeted disruption of the biglycan gene leads to an osteoporosis-like phenotype in mice. *Nat. Genet.* **20**, 78–82 (1998).
28. M. Ito, Y. Ehara, J. Li, K. Inada, K. Ohno, Protein-anchoring therapy of biglycan for *Mdx* mouse model of Duchenne muscular dystrophy. *Hum. Gene Ther.* **28**, 428–436 (2017).
29. B. Manori, A. Vaknin, P. Vaňková, A. Nitzan, R. Zaidel-Bar, P. Man, M. Giladi, Y. Haitin, Chloride intracellular channel (CLIC) proteins function as fusogens. *Nat. Commun.* **15**, 2085 (2024).
30. B. Ponsioen, L. van Zeijl, M. Langeslag, M. Berryman, D. Littler, K. Jalink, W. H. Moolenaar, Spatiotemporal regulation of chloride intracellular channel protein CLIC4 by RhoA. *Mol. Biol. Cell* **20**, 4664–4672 (2009).
31. J. Aggelidakis, A. Berdiaki, D. Nikitovic, A. Papoutsidakis, D. J. Papachristou, A. M. Tsatsakis, G. N. Tzanakakis, Biglycan regulates MG63 osteosarcoma cell growth through a LPR6/β-Catenin/IGFR-IR signaling axis. *Front. Oncol.* **8**, 470 (2018).
32. K. I. Watt, K. F. Harvey, P. Gregorevic, Regulation of tissue growth by the mammalian hippo signaling pathway. *Front. Physiol.* **8**, 942 (2017).
33. V. Fu, S. W. Plouffe, K. L. Guan, The Hippo pathway in organ development, homeostasis, and regeneration. *Curr. Opin. Cell Biol.* **49**, 99–107 (2018).
34. T. H. Chen, C. Y. Chen, H. C. Wen, C. C. Chang, H. D. Wang, C. P. Chuu, C. H. Chang, YAP promotes myogenic differentiation via the MEK5-ERK5 pathway. *FASEB J.* **31**, 2963–2972 (2017).

35. K. I. Watt, D. C. Henstridge, M. Ziemann, C. B. Sim, M. K. Montgomery, D. Samocha-Bonet, B. L. Parker, G. T. Dodd, S. T. Bond, T. M. Salmi, R. S. Lee, R. E. Thomson, A. Hagg, J. R. Davey, H. Qian, R. Koopman, A. El-Osta, J. R. Greenfield, M. J. Watt, M. A. Febbraio, B. G. Drew, A. G. Cox, E. R. Porrello, K. F. Harvey, P. Gregorevic, Yap regulates skeletal muscle fatty acid oxidation and adiposity in metabolic disease. *Nat. Commun.* **12**, 2887 (2021).
36. J. Y. Seo, J. S. Kang, Y. L. Kim, Y. W. Jo, J. H. Kim, S. H. Hann, J. Park, I. Park, H. Park, K. Yoo, J. Rhee, J. W. Park, Y. C. Ha, Y. Y. Kong, Maintenance of type 2 glycolytic myofibers with age by Mib1-Actn3 axis. *Nat. Commun.* **12**, 1294 (2021).
37. I. Grabowska, A. Szeliga, J. Moraczewski, I. Czaplicka, E. Brzóska, Comparison of satellite cell-derived myoblasts and C2C12 differentiation in two- and three-dimensional cultures: Changes in adhesion protein expression. *Cell Biol. Int.* **35**, 125–133 (2011).
38. Y. Yu, Y. Su, G. Wang, M. Lan, J. Liu, R. Garcia Martin, B. B. Brandao, M. Lino, L. Li, C. Liu, C. R. Kahn, Q. Meng, Reciprocal communication between FAPs and muscle cells via distinct extracellular vesicle miRNAs in muscle regeneration. *Proc. Natl. Acad. Sci. U.S.A.* **121**, e2316544121 (2024).
39. M. Shang, F. Cappellesso, R. Amorim, J. Serneels, F. Virga, G. Eelen, S. Carobbio, M. Y. Rincon, P. Maechler, K. De Bock, P. C. Ho, M. Sandri, B. Ghesquière, P. Carmeliet, M. Di Matteo, E. Berardi, M. Mazzone, Macrophage-derived glutamine boosts satellite cells and muscle regeneration. *Nature* **587**, 626–631 (2020).
40. D. Xu, B. Wan, K. Qiu, Y. Wang, X. Zhang, N. Jiao, E. Yan, J. Wu, R. Yu, S. Gao, M. Du, C. Liu, M. Li, G. Fan, J. Yin, Single-cell RNA-sequencing provides insight into skeletal muscle evolution during the selection of muscle characteristics. *Adv. Sci.* **10**, e2305080 (2023).
41. F. Yue, P. Bi, C. Wang, J. Li, X. Liu, S. Kuang, Conditional loss of Pten in myogenic progenitors leads to postnatal skeletal muscle hypertrophy but age-dependent exhaustion of satellite cells. *Cell Rep.* **17**, 2340–2353 (2016).
42. V. D. Soleimani, V. G. Punch, Y. Kawabe, A. E. Jones, G. A. Palidwor, C. J. Porter, J. W. Cross, J. J. Carvajal, C. E. Kockx, W. F. van IJcken, T. J. Perkins, P. W. Rigby, F. Grosveld, M. A. Rudnicki, Transcriptional dominance of pax7 in adult myogenesis is due to high-affinity recognition of homeodomain motifs. *Dev. Cell* **22**, 1208–1220 (2012).
43. M. C. Sincennes, C. E. Brun, M. A. Rudnicki, Concise review: Epigenetic regulation of myogenesis in health and disease. *Stem Cells Transl. Med.* **5**, 282–290 (2016).
44. J. Von Maltzahn, A. E. Jones, R. J. Parks, M. A. Rudnicki, Pax7 is critical for the normal function of satellite cells in adult skeletal muscle. *Proc. Natl. Acad. Sci. U.S.A.* **110**, 16474–16479 (2013).
45. S. Günther, J. Kim, S. Kostin, C. Lepper, C. M. Fan, T. Braun, Myf5-positive satellite cells contribute to Pax7-dependent long-term maintenance of adult muscle stem cells. *Cell Stem Cell* **13**, 590–601 (2013).
46. K. Zhang, Y. Zhang, L. Gu, M. Lan, C. Liu, M. Wang, Y. Su, M. Ge, T. Wang, Y. Yu, C. Liu, L. Li, Q. Li, Y. Zhao, Z. Yu, F. Wang, N. Li, Q. Meng, Islr regulates canonical Wnt signaling-mediated skeletal muscle regeneration by stabilizing Dishevelled-2 and preventing autophagy. *Nat. Commun.* **9**, 5129 (2018).
47. D. P. Millay, J. R. O'Rourke, L. B. Sutherland, S. Bezprozvannaya, J. M. Shelton, R. Bassel-Duby, E. N. Olson, Myomaker is a membrane activator of myoblast fusion and muscle formation. *Nature* **499**, 301–305 (2013).



**Acknowledgments**

**Funding:** This work was supported by National Key Research and Development Program of China (grant 2021YFF1000603) and National Natural Science Foundation of China (grants 31790412 and 32372898). **Author Contributions:** Conceptualization: J.Y. and X. Zhang. Data curation: J.Y. Formal analysis: J.Y., X. Zhang., L.H., and L.W. Funding acquisition: J.Y. and X. Zhang. Investigation: J.Y., X. Zhang., L.H., and L.W. Methodology: J.Y., X. Zhang., L.H., and L.W. Project administration: J.Y. Resources: J.Y., X. Zhang., L.H., L.W., Y.W., E.Y., B.W., Q.Z., and P.Z. Supervision: J.Y. Validation: J.Y., X. Zhang., L.H., and L.W. Visualization: J.Y. and X. Zhang. Writing—original draft: J.Y. and X. Zhang. Writing—review and editing: J.Y., X. Zhang., and X. Zhao. **Competing interests:** The authors declare that they have no competing interests. **Data and materials availability:** All data needed to evaluate the conclusions in the paper are present in the paper and/or the Supplementary Materials.

Submitted 25 May 2024
Accepted 10 September 2024
Published 11 October 2024
10.1126/sciadv.adq6795